Accepted Manuscript

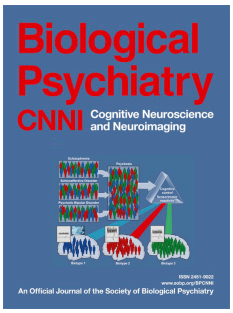

Insula functional connectivity in schizophrenia: Subregions, gradients and symptoms

Ye Tian, Andrew Zalesky, Chad Bousman, Ian Everall, Christos Pantelis

PII: S2451-9022(18)30325-2

DOI: https://doi.org/10.1016/j.bpsc.2018.12.003

Reference: BPSC 365

To appear in: *Biological Psychiatry: Cognitive Neuroscience and Neuroimaging*

Received Date: 12 October 2018

Revised Date: 26 November 2018

Please cite this article as: Tian Y., Zalesky A., Bousman C., Everall I. & Pantelis C., Insula functional connectivity in schizophrenia: Subregions, gradients and symptoms, *Biological Psychiatry: Cognitive Neuroscience and Neuroimaging* (2019), doi: https://doi.org/10.1016/j.bpsc.2018.12.003.

Title Page

Insula functional connectivity in schizophrenia:

Subregions, gradients and symptoms

Ye Tian [a], Andrew Zalesky [a,b], Chad Bousman [a,e,f], Ian Everall [e,g] , Christos Pantelis [a,c,d,e]

[a] Melbourne Neuropsychiatry Centre, Department of Psychiatry, The University of Melbourne and Melbourne Health, Carlton South, VIC, Australia

[b] Department of Biomedical Engineering, The University of Melbourne, Parkville, VIC, Australia

[c] Florey Institute for Neuroscience and Mental Health, Australia

[d] Centre for Neural Engineering, The University of Melbourne, Australia

[e] The Cooperative Research Centre for Mental Health, Australia

[f] Department of Medical Genetics, Psychiatry, Physiology and Pharmacology, University of Calgary, Canada.

[g] Institute of Psychiatry, Psychology, and Neuroscience, King's College London, United Kingdom

Location of work and address for reprints:

Dr Ye Tian

Melbourne Neuropsychiatry Centre

Level 3, Alan Gilbert Building, 161 Barry Street

The University of Melbourne, Carlton South, VIC 3053, Australia

Phone: +61 3 9035 8637

Email: yetianmed@gmail.com

Running title: Connectional pathology of insula in schizophrenia

Key words: Insular cortex; Schizophrenia; Clustering; Resting-state fMRI; Parcellation; Diversity curve

Word count (text): 4426 *Abstract word count:* 249

Number of Figures: 4 *Number of Tables:* 1

Number of References: 73

Number of Supplementary Material: 1

Abstract

Background: The insular cortex is connected to a diverse network of cortical and subcortical areas. This study aims to investigate whether the diversity in functional connectivity across the insula's topography is altered in schizophrenia and relates to the disorder's clinical symptoms.

Methods: Insula-to-whole-brain functional connectivity was mapped using resting-state functional MRI at the resolution of voxels in individuals with schizophrenia (*N*=49) and healthy comparison individuals (*N*=52). Diversity in functional connectivity across the insula's topography was represented as: i) discrete subregions; and, ii) gradients of continuous variation. Canonical correlation analysis (CCA) was used to relate inter-individual variation in insula connectivity with clinical symptoms.

Results: Insula connectional diversity was parcellated into two subregions: dorsal-anterior and ventral-posterior. Differentiation in connectivity profiles between these subregions was significantly reduced in the schizophrenia group. Compared to the control group, insula functional connectivity was overall reduced in schizophrenia. A significant interaction effect between diagnosis and insula subregion indicated that the anterior subregion in schizophrenia was connected with increased strength to the somatosensory, motor, occipital and parietal cortices, whereas the posterior subregion showed increased connectivity with the thalamus and prefrontal cortex. Insula connectivity with the anterior cingulate and auditory cortices significantly associated with cognitive impairment, negative symptoms, poor psychosocial functioning and duration of illness (r = 0.64, p = 0.03).

Conclusions: Diversity in functional connectivity across the insula's rostro-caudal axis is reduced in schizophrenia, resulting in reduced differentiation between anterior and posterior

insula. Inter-individual variation in insula connectivity explains variability in some of the disorder's clinical symptoms.

Introduction

Functional dysconnectivity of the insular cortex is consistently observed in psychosis spectrum disorders, including individuals with first-episode psychosis (1-3), chronic schizophrenia (4, 5) and individuals at high risk for the disorder (6-8). Specifically, the insula shows aberrant patterns of connectivity with the cingulate cortex as well as regions comprising the default mode network (DMN) and central executive network (CEN) (4-7). Most previous neuroimaging studies investigating the connectivity of the insula in schizophrenia have treated the insula as a single, homogeneous region (3), or have only considered its anterior aspect (4, 5, 7-9). In particular, neuroimaging data are typically averaged over all voxels comprising the insula to provide a summary characterization, and thus any potential variation in connectivity across the topography (spatial extent) of the insula is potentially overlooked. We refer to this topographic variation as connectional diversity. A region with greater connectional diversity shows greater variation across its topography with respect to the cortical and subcortical regions to which it connects.

Recently, functional and structural magnetic resonance imaging (MRI) studies have sought to characterize the insula's connectional diversity using one of two models: i) discrete subregions (clusters) (10); and; ii) continua of variation (diversity curves) (11). These studies have generally been limited to healthy individuals. According to the subregions model, the insula can be parcellated into clusters, where each cluster is associated with a distinct connectivity pattern. Many studies employing the subregions model suggest that the insula is best represented with a bipartite subdivision comprising anterior and posterior subregions (10, 12-16), while other studies provide evidence of a tripartite clustering in which the anterior insula is further subdivided into dorsal and ventral components (4, 17, 18), as well as

parcellations comprising more than three subdivisions (14, 19-27). Particular subregions have been linked to specific aspects of cognition, emotion and somatosensory sensations (18, 28, 29). More recently, it has been suggested that the insula's connectional diversity can be represented more parsimoniously as a continuum of gradual variation along a rostro-caudal axis, rather than with discrete subregions (30). Inter-individual variation in the rate of variation along this axis of the insula has been found to explain significant variation in behavioral traits assessed in healthy adults (11).

The aim of the present study was to characterize the diversity in functional connectivity across the topography of the insular cortex in adults with schizophrenia. To this end, we acquired resting-state functional MRI (fMRI) data in individuals with schizophrenia and healthy comparisons individuals, and used these data to map the functional connectivity profile of each insula voxel with respect to all other cortical and subcortical voxels. We clustered insula voxels into distinct subregions based on similarity in their connectivity profiles, and also modelled variation in connectivity among insula voxels continuously using the recently proposed concept of a diversity curve. An individual's diversity curve quantifies how rapidly the insula's connectivity with the rest of the cortex changes per unit length along the insula's rostro-caudal axis (11). We then performed statistical analyses to compare the functional connectivity profiles of distinct insula subregions between the schizophrenia and healthy comparison groups. Finally, we assessed whether patterns of insula functional connectivity in the schizophrenia group associated with inter-individual variation in the severity of psychosis symptoms, cognition and psychosocial functioning. Given the widespread reductions in functional connectivity previously reported in this cohort (31), and the known association between insula connectional diversity and cognitive-affective function (11), we hypothesized that schizophrenia would be associated with reduced insula connectional diversity and reduced segregation (differentiation) between the connectivity

profiles of putative insula subregions. Our hypothesis is supported by evidence of reduced segregation at the global scale of whole-brain functional networks in the disorder (32) as well as loss of functional specialization within specific areas such as the prefrontal cortex (33). This is the first study to comprehensively characterize connectional pathology across the topography of the insula in individuals with schizophrenia.

Methods and Materials

Participants, Image Acquisition and Image Preprocessing

Participants: Individuals with established schizophrenia (*N*=49, mean age: 41.02 ± 9.93, 15 females) and healthy comparison individuals matched for average age, sex and handedness (*N*=52, mean age: 39.85 ± 10.46, 17 females) were included in this study. The majority of individuals with schizophrenia (*N*=44) were considered resistant to treatment (34) and currently prescribed and taking clozapine. The diagnosis of schizophrenia was further confirmed by the Mini International Neuropsychiatric Interview (MINI) (35). Healthy comparison individuals were recruited from the local community. Individuals satisfying at least one of the following exclusion criteria were not considered: current or history of psychiatric diagnoses, substance dependence, mental retardation (IQ < 70), first-degree relatives with psychiatric illness, neurological disorders, impaired thyroid function, diabetes and other major medical conditions. This study was approved by the Melbourne Health Human Research Ethics Committee (MHREC ID 2012.069). All participants gave written consent prior to participation.

The severity of clinical symptoms was assessed using the Positive and Negative Syndrome Scale (PANSS) (36), Scale for the Assessment of Positive Symptoms (SAPS) (37) and Scale for Assessment of Negative Symptoms (SANS) (38) on the day of screening. For all individuals, social, occupational, and psychological functioning were measured with the

Global Assessment of Functioning (GAF) (39), Social and Occupational Functioning Assessment Scale (SOFAS) (40) and Wechsler Abbreviated Scale of Intelligence (WASI) for cognition (41) (Table 1). Antipsychotic dosage was converted to chlorpromazine equivalent dose using an established conversion methodology (42).

Image acquisition and resting-state fMRI data preprocessing are described in Supplementary Material.

Insula Discrete Subregions Model

Cluster Analysis: For each individual, the left and right insula were separately parcellated into distinct subregions using cluster analysis. In brief, functional connectivity was mapped between each insula voxel and all other gray matter voxels, and Ward's linkage was then used to cluster insula voxels according to similarity in connectional profiles. The morphology of the resulting clusters (i.e. volume and length measurements) was then tested for differences between the schizophrenia and healthy comparison group using the Wilcoxon rank sum test. Functional connectivity mapping and cluster analysis is described in detail in Supplementary Material. Modularity analysis (Newman's spectral community detection algorithm) was used to combine each individual's insula parcellation to generate a group-level consensus parcellation of the insula for each of the two groups. The modularity Q-score was then used to test whether the degree of differentiation in functional connectivity profiles between the anterior and posterior insula subregions differed between the two groups (Supplementary Material).

Whole-brain functional connectivity profile of insula subregions: Using the cluster analysis described above, we found that the insula was most parsimoniously partitioned into two clusters for the majority of schizophrenia (88%) and healthy comparison (87%) individuals. While substantial variation in the shape and location of clusters across individuals was evident (Supplementary Figure S1), the group-level consensus parcellation comprised two

modules that mapped to anterior and posterior insula subregions. We sought to test whether whole-brain functional connectivity patterns differed between anterior and posterior insula, or between the schizophrenia and healthy comparison groups. To this end, the intersection between the separate anterior and posterior insula masks for each group was computed to yield a single anterior and posterior insula mask that was common to both groups (Figure 1C & Supplementary Table S1). For each individual, the fMRI signal was averaged across all voxels comprising the anterior and posterior mask and this averaged signal was then correlated (Pearson correlation) with all other gray matter voxels, yielding a whole-brain anterior and posterior insula functional connectivity map for each person. For each gray matter voxel comprising this map, within-subjects analysis of variance (ANOVA) was used to test the main effects of diagnosis (schizophrenia/control), subregion (anterior/posterior), and laterality (left/right) on insula connectivity, as well as the interaction between diagnosis and the latter two main effects. Nonparametric cluster-based inference, as implemented in Randomise (43), was used to control the familywise error (FWE) across the set of all voxels and to identify voxel clusters for which the main or interaction effects were significant (permutations: n=10,000; cluster forming threshold: t=2.5, p <0.05).

Insula Continuum Model and Diversity Curves

It has recently been suggested that connectional diversity across the insula's topography is more parsimoniously represented as continua of gradual variation, rather than with discrete subregions (11). Given this consideration, we employed the recently proposed concept of a diversity curve (11) to represent the insula's connectional diversity for each individual as a continuum of variation. In brief, Laplacian eigenmaps (44) were mapped for each individual's insula using established methods (45) and the eigenmaps were projected onto a rostro-caudal curvilinear trajectory through the insula representing the trajectory of maximal change in the eigenmap (11). This yielded a separate diversity curve for each individual.

Further details are provided in Supplementary Material. We compared the diversity curves between the schizophrenia and healthy comparison groups to test the hypothesis that schizophrenia would be associated with a reduction in insula connectional diversity. To this end, a two-sample *t*-test was performed to test for a difference in diversity between the schizophrenia and healthy comparison individuals at each point along the diversity curves. The false discovery rate (FDR) was used to control for multiple comparisons across the set of all points.

Clinical Associations

We hypothesized that inter-individual variation in the extent of insula connectivity reductions with the anterior cingulate cortex (ACC) and superior temporal gyrus (STG), would associate with clinical severity in the schizophrenia group. This hypothesis is supported by suggestions that: i) the ACC and anterior insula are key regions of the salience network (28), which is known to show aberrant network switching in schizophrenia (5, 46); and, ii) the STG is crucial for language (Wernicke's area) and auditory (Heschl's gyrus and planum temporale) processing, and dysconnectivity of this region is associated with auditory hallucinations in the disorder (47-49). To test this hypothesis, for each individual with schizophrenia, fMRI data were averaged across all voxels comprising the ACC and STG clusters identified with Randomise as well as the masks delineating the posterior and anterior insula subregions. Note that the ACC cluster identified with Randomise included a portion of the supplementary motor area (SMA), and thus we refer to this cluster as ACC/SMA. The resulting regionally-averaged time series were then correlated (Pearson correlation) to yield functional connectivity estimates between: i) anterior insula and ACC; and; ii) posterior insula and STG. Finally, canonical correlation analysis (CCA) (50) was used to test for a multivariate association between these two functional connectivity estimates and several measures of

symptom severity; namely, measures derived from the following instruments: PANSS, SAPS, SANS, GAF, SOFAS, WASI and duration of illness (DOI) (Supplementary Material).

Numeric computation was performed in MATLAB R2017b. Images were visualized using BrainNetViewer1.6 (51) and FslView software (http://fsl.fmrib.ox.au.uk/fsl/fslwiki/FslView).

Results

Demographic and clinical characteristics are shown in Table 1. The schizophrenia and healthy comparison groups were matched in terms of mean age, sex and handedness, and thus these factors were not controlled when performing group comparisons. However, IQ and measures of social and general functioning were significantly reduced in the schizophrenia group.

Reduced Differentiation Between Anterior and Posterior Insula Subregions

Bipartite parcellation of the insula into anterior and posterior subregions yielded the most parsimonious representation in the majority of individuals with schizophrenia (88%) and healthy comparison individuals (87%). For the remaining individuals, insula voxels were partitioned into two clusters according to the individual's best fitting bipartite solution. To facilitate between-group comparison, only bipartite insula parcellations were analyzed here. The volume (cluster size) of each insula subregion was estimated by enumerating the number of voxels assigned to the cluster of voxels delineating each subregion and multiplying this number by the volume of each individual voxel ($8\times10^{-3}cm^3$). The anterior insula subregion was significantly reduced in the schizophrenia group (right: z=3.81, schizophrenia: 4.59 ± 2.2 cm^3, comparison group: 6.41 ± 2.2 cm^3, p <0.001; left: z=4.47, p <0.001), while the posterior insula was significantly increased (right: z=3.44, schizophrenia: 5.60 ± 2.3 cm^3, comparison group: 4.40 ± 2.2 cm^3, p <0.001; left: z=3.92, p <0.001) and extended further anteriorly (right: z=3.89, p <0.001; left: z=3.13, p=0.0017) and laterally (right: z=3.89, p

<0.001; left: z=3.87, p <0.001), relative to the healthy comparison group (Supplementary Figure S2).

We found that the differentiation between these two putative insula subregions was significantly reduced in the schizophrenia group (Q-score right insula, schizophrenia: 0.13, comparison group: 0.20, p=0.0038, Figure 1A & B; Q-score left insula: schizophrenia: 0.12, comparison group: 0.21, p=0.002, Supplementary Figure S3).

Altered Insula Functional Connectivity

Having parcellated the insula into two distinct subregions (anterior and posterior), we next sought to investigate whether the functional connectivity between these two subregions and the rest of the cortex was altered in schizophrenia. We investigated three main effects (subregion, diagnosis, laterality) and two interaction effects (diagnosis × subregion, diagnosis × laterality). We identified regional clusters associated with each of these effects.

Main effect of subregion (anterior vs posterior): Across all individuals (schizophrenia and healthy comparison individuals combined), we found that the anterior insula was preferentially connected to the fronto-limbic and paralimbic areas (peak t=24.2, p <0.001), and the posterior cerebellar lobes (crus I and crus II) (peak t=8.17, p=0.006), whereas the posterior insula was characterized by extensive parieto-temporo-occipital and anterior cerebellar connectivity (peak t=22.4, p <0.001; Figure 2A).

Main effect of diagnosis (schizophrenia vs healthy comparison group): Functional connectivity was significantly reduced in the schizophrenia group between the insula and multiple cortical/subcortical areas. Specifically, schizophrenia was associated with significant reductions in connectivity between the anterior insula and regions located at the bilateral ACC, SMA, paracingulate cortex and superior frontal gyrus (peak t=5.51, p=0.0118), as well as regions in the frontal and central operculum, orbitofrontal cortex, inferior frontal gyrus, temporal pole, ventral medial prefrontal cortex (vmPFC), and subcortical areas such as the

amygdala, putamen, parahippocampal gyrus and pallidum (peak t=5.7, p=0.0035) (Figure 2B, upper panel). In contrast, the posterior insula showed significantly reduced connectivity with the bilateral STG, planum temporale, Heschl's gyrus, middle temporal gyrus and parietal and central operculum (right cluster: peak t=5.31, p=0.0018; left cluster: peak t=4.59, p=0.0091). Furthermore, functional connectivity between the posterior insula and the bilateral precentral and postcentral gyrus, posterior and anterior cingulate cortex, precuneus, and SMA was significantly reduced in the schizophrenia group (peak t=5.4, p=0.0018) (Figure 2B, lower panel). Significant increases in connectivity were not found in the schizophrenia group (p > 0.05).

Main effect of laterality (left vs right): While the insula's cerebral connections showed an ipsilateral preference (anterior: peak t=16.8, p <0.001; posterior: peak t=17.9, p <0.001), the insula was more extensively connected to the cerebellum in the contralateral hemisphere (peak t=4.68, p=0.025) (Supplementary Figure S5).

Interaction effect (diagnosis × subregion): A significant interaction was found between diagnosis and subregion. More specifically, the anterior insula in the schizophrenia group showed increased connectivity with the precentral and postcentral gyrus (i.e. primary motor and somatosensory cortex; peak t=5.3, p=0.001), occipital cortex and anterior lobe of the cerebellum (peak t=5.34, p < 0.001), and a cluster located in the primary/secondary auditory cortices (peak t=4.99, p=0.023). In contrast, the posterior insula in the schizophrenia group showed increased connectivity to the prefrontal cortex (peak t=4.37, p=0.04), bilateral thalamus (peak t=5.27, p=0.036), pons and posterior cerebellar lobes (peak t=5.75, p=0.017). Comparable findings were evident for the left insula (Supplementary Figure S4).

Interaction effect (diagnosis × laterality): No significant interaction was found between diagnosis and laterality, suggesting that the disorder does not preferentially affect the left or right insula.

Diversity Curves

Diversity curves based on Fielder eigenvectors were mapped for each individual to continuously characterize the rate at which the insula's connectional profile to the rest of the cortex changed along the insula's rostro-caudal axis. Figure 3A shows group-averaged diversity curves for the schizophrenia (green curve) and healthy comparison groups (blue curve). Consistent with previous work (11), the diversity curves show a relatively constant slope, suggesting that the insula's connectivity profile varies gradually and continuously across its topography, from dorsal-posterior to ventral-anterior. The connectional diversity for the schizophrenia group was reduced in the anterior portion of the insula, indicated by a reduction in the diversity curve's slope (dashed box in Figure 3A); however, this between-group difference did not survive correction for multiple comparisons ($p < 0.05$, Figure 3A). Group-consensus eigenmaps were projected to insula voxels in MNI space to enable anatomical visualization (Figure 3B).

Clinical Associations

Canonical correlation analysis identified a significant mode of covariance between inter-individual variation in nine measures of disorder severity and two measures of insula functional connectivity ($r = 0.64$, $p = 0.03$; FWE corrected; Figure 4A). The canonical coefficients for each of the two functional connectivity estimates (Figure 4B) quantify the extent to which each of two connectivity estimates contributed to the significant mode of covariance. Figure 4C shows that IQ, GAF and SOFAS are positively correlated with the significant mode of covariance, whereas SANS, PANSS-NEG and DOI are negative. Therefore, higher insula functional connectivity with the ACC/SMA and STG was associated with higher IQ and psychosocial functioning (i.e. GAF and SOFAS) as well as less severity of psychotic symptoms (SANS and PANSS-NEG) and shorter duration of illness (DOI). Conversely, individuals with lower insula functional connectivity with the ACC/SMA and

STG are more likely to show poorer cognitive performance, psychosocial functioning as well as more severe psychotic symptoms and longer illness duration. In supplementary analyses, an exploratory CCA was conducted on the other six regions found to show significant functional connectivity reductions with the insula in the schizophrenia group (Table S2). The exploratory CCA did not identify any significant associations between inter-individual variation in symptoms and insula functional connectivity among this broader set of regions.

Inter-individual variation in age, sex and antipsychotic dose (chlorpromazine equivalent dose) did not associate with functional connectivity between the insula and eight clusters (Table S2) found to show significantly reduced connectivity with the insula in the schizophrenia group. Table S3 shows test statistics and p-values for each of these 3 (age, sex, CPZ) × 8 (clusters) = 24 tests.

Discussion

This study comprehensively characterized the functional connectivity architecture of the insular cortex in individuals with schizophrenia. Unlike previous functional connectivity studies of the insula in schizophrenia, rather than treating the insula as a single, homogeneous region, or only considering its anterior aspect, we specifically focussed on investigating how the insula's connectivity with the rest of the cortex varied across its topography (i.e. across its spatial extent). The insular cortex is a connectionally diverse region, in that its most dorsal-posterior extremity connects with markedly different cortical and subcortical areas compared to its ventral-anterior aspect (11). In this study, we aimed to determine whether this connectional diversity was aberrant in schizophrenia. We found that the connectivity profiles of the anterior and posterior insula were less well differentiated in schizophrenia, and that the extent of reduction in connectivity between insula subregions and key regions of the salience

network and auditory cortex were associated with inter-individual variation in symptom severity.

Our initial clustering analysis suggested that the insula was most parsimoniously parcellated into two subregions in the majority of schizophrenia and healthy comparison individuals. Volumetrically, we found that the posterior insula subregion was significantly larger in the schizophrenia group, while the anterior insula was significantly reduced, relative to the healthy comparison group. It is important not to confuse these volumetric differences with previous studies reporting that schizophrenia is associated with reduced insula gray matter volume, particularly the anterior aspect of the insula (52-56). We used a common mask to delineate the insula in all individuals, and thus we did not model any potential inter-individual variation in the entire insula volume. The volumetric differences found in the present study relate to segregation of functional connectivity (57-59) and are not necessarily related to gray matter morphology. In particular, the increased volume of the posterior insula subregion suggests that the characteristic connectivity profile of the posterior insula encompasses a larger share of the insula's entire volume in individuals with schizophrenia. This is at the expense of the anterior insula occupying a smaller volume.

We found that the differentiation between the anterior and posterior insula subregions was significantly reduced in the schizophrenia group, relative to the healthy comparison group, as quantified by the modularity *Q*-score. This suggests that the connectional diversity of the insula is reduced in schizophrenia; namely, the network of areas with which the anterior insula connects is less well differentiated from the network of areas with which the posterior insula connects. In fact, differentiation between the anterior and posterior insula was only marginally higher than chance level in the schizophrenia group ($Q \approx 0.1$). Specifically, anterior insula subregion preferentially connects to the frontal-limbic/paralimbic areas and cerebellar non-motor regions, whereas the posterior subregion shows extensive connectivity

with the parieto-temporo-occipital lobe and motor regions of cerebellum. This anterior-posterior subdivision is consistent with previous functional/diffusional parcellation studies in humans (10, 12, 13, 15, 60, 61), and axonal tracing studies in macaques (62, 63).

We found that functional connectivity between the insula and multiple cortical and subcortical areas as well as the cerebellum was significantly reduced in the schizophrenia group. Many of the areas affected comprise cognitive networks (20, 21) and are associated with a wide range of cognitive, affective, and sensory-motor functions that are disturbed in schizophrenia (64-66). We found a significant interaction in the connectivity profiles between diagnosis (schizophrenia vs healthy comparison group) and insula subregion (anterior vs posterior). In the schizophrenia group, the anterior insula connected with increased strength to regions that are normally connected with the posterior insula (i.e. the precentral/postcentral gyrus, occipital/parietal cortex and anterior cerebellar lobe). Conversely, the posterior insula showed increased connectivity in schizophrenia with regions that are preferentially connected with the anterior insula in healthy individuals (i.e. prefrontal cortex, thalamus and posterior cerebellar lobe. This interaction effect suggests that the connectivity profiles of the anterior and posterior insula are less well differentiated in schizophrenia, consistent with lack of insula connectional diversity in the disorder.

Using the recently developed concept of a diversity curve (11), we found that the insula's connectional diversity varied gradually along a rostro-caudal axis in both the schizophrenia and healthy comparison groups. Furthermore, we found no evidence of a discrete boundary between putative insula subregions, which would have been evidenced by an abrupt change in the diversity curve slope. It is important to remark that while we did not find any evidence of discrete insula subregions, modelling the insula's connectional diversity with subregions can nevertheless provide meaningful insight. Discrete approximations can simplify continuous systems which in turn facilitates inference and more intuitive interpretations. For

example, mapping of neural connectomes mandates the delineation of discrete subregions to serve as network nodes (67). Anterior and posterior insula subregions can thus represent distinct nodes in connectomic studies. Insula diversity curves for the schizophrenia group were reduced within an anterior portion of the insula; however, this between-group difference did not survive correction for multiple comparisons. Within the anterior portion of the insula implicated (dashed box, Figure 3A), the diversity curve's slope showed a trend toward reduction in the schizophrenia group, which may suggest that this portion of the insula is abnormally homogeneous in the disorder.

Importantly, we found that the reduced functional connectivity between anterior insula and ACC including SMA, known as the salience network and the functional connectivity between posterior insula and the language and auditory cortex (STG, Heschl's gyrus, planum temporale and Wernicke's area) were associated with poor clinical outcomes including cognitive impairment and general social and occupational functioning as well as the severity of symptoms, particularly negative symptoms. Our findings support the emerging hypothesis that the salience network is significantly involved in the pathophysiology of psychosis (7, 46, 68, 69) particularly with respect to disturbances in the integration of sensory perception facilitated by the posterior insula (68). Of note, reduced insula functional connectivity was also associated with longer illness duration, suggesting progressive deterioration of connectivity over the course of illness, although longitudinal neuroimaging would be required to confirm this suggestion. We therefore conclude that impaired functional connectivity between the insula and these key regions may be a determinant of disorder severity.

Limitations

First, our sample is moderate in size and our fMRI data is of poorer spatial and temporal resolution compared to the data used in our previous analysis of the insula in healthy

individuals (11). Second, although antipsychotic dose was not correlated with any of the functional connectivity effects reported in this study, medication cannot be excluded as a potential confound (70-72). Interestingly, analysis of functional connectivity during a salience attribution task indicated that schizophrenia-related reductions in connectivity between the insula and ACC were only evident in the subgroup of untreated individuals with first-episode psychosis, but not in the medicated subgroup (72). However, these findings require replication, given the small size of the medicated subgroup. Finally, IQ was significantly reduced in the schizophrenia group, representing a potential confounding effect on the neuroimaging findings reported in our study. However, it is generally difficult to disentangle low IQ from the illness because of the widespread neurocognitive deficits evident in the majority of individuals with schizophrenia (65), and controlling for IQ as part of statistical inference may be considered inappropriate for this reason (73).

Conclusions

Using resting-state fMRI, we comprehensively characterized functional connectivity across the topography of the insular cortex in individuals with schizophrenia. We represented the insula's connectional diversity using discrete subregions (anterior and posterior) as well as a continuum of gradual variation. We found that the anterior and posterior insula subregions were connected to distinct cortical and subcortical regions in the healthy comparison individuals. However, in the schizophrenia group, this distinction in the connectivity profiles of the anterior and posterior insula was significantly reduced, suggesting a lack of segregation between these two subregions in the disorder. This was evidenced by a significant interaction between diagnosis and subregion, whereby the anterior insula showed increased connectivity with somatosensory/motor, occipital/parietal cortices and motor regions of cerebellum in schizophrenia, whereas the connectivity between the posterior insula and prefrontal cortex, thalamus and cerebellar non-motor region was stronger. Insula

diversity curves suggested that the anterior insula may be abnormally homogeneous in the schizophrenia group. Finally, we found that impaired insula functional connectivity was associated with inter-individual variation in cognitive deficits, psychotic symptoms and psychosocial functioning. We conclude that the anterior and posterior insula show differential connectivity profiles, but this differentiation is reduced in schizophrenia, resulting in reduced connectional diversity across the insula and possibly contributing to the disorder's psychotic symptoms. Future research may focus on mapping the subregional architecture of the insular cortex as a function of age using longitudinal neuroimaging data. This would establish the age range during which the connectivity profiles of the anterior and posterior insula significantly differentiate, and whether this differentiation is evident before the onset of psychosis.

Acknowledgements

The authors wish to acknowledge the CRC Scientific Advisory Committee, in addition to the contributions of study participants, clinicians at recruitment services, staff at the Murdoch Children's Research Institute, staff at the Australian Imaging, Biomarkers and Lifestyle Flagship Study of Aging, and research staff at the Melbourne Neuropsychiatry Centre, including coordinators Phassouliotis, C., Merritt, A., and research assistants, Burnside A., Cross, H., Gale, S., and Tahtalian, S.

Funding

Y.T. was supported by the China Scholarship Council – University of Melbourne Research Scholarship. A.Z. was supported by the Australian National Health and Medical Research Council (NHMRC) Senior Research Fellowship B (ID: 1136649). C.P. was supported by NHMRC Senior Principal Research Fellowship (ID: 628386 & 1105825).

Conflict of interest: None declared.

Disclosures unrelated to the current study: Christos Pantelis has participated on Advisory Boards for Janssen-Cilag, Astra-Zeneca, Lundbeck, and Servier. He has received honoraria for talks presented at educational meetings organised by Astra-Zeneca, Janssen-Cilag, Eli-Lilly, Pfizer, Lundbeck and Shire. All are unrelated to the current study. All other authors report no biomedical financial interests or potential conflicts of interest.

References

1. Kasparek T, Prikryl R, Rehulova J, Marecek R, Mikl M, Prikrylova H, et al. (2013): Brain functional connectivity of male patients in remission after the first episode of schizophrenia. *Human brain mapping*. 34:726-737.
2. Mallikarjun PK, Lalousis PA, Dunne TF, Heinze K, Reniers RL, Broome MR, et al. (2018): Aberrant salience network functional connectivity in auditory verbal hallucinations: a first episode psychosis sample. *Translational psychiatry*. 8:69.
3. Pang L, Kennedy D, Wei Q, Lv L, Gao J, Li H, et al. (2017): Decreased Functional Connectivity of Insular Cortex in Drug Naïve First Episode Schizophrenia: In Relation to Symptom Severity. *PloS one*. 12.
4. Moran LV, Tagamets MA, Sampath H, O'Donnell A, Stein EA, Kochunov P, et al.

(2013): Disruption of anterior insula modulation of large-scale brain networks in schizophrenia. *Biological psychiatry*. 74:467-474.
5. Palaniyappan L, Simmonite M, White TP, Liddle EB, Liddle PF (2013): Neural primacy of the salience processing system in schizophrenia. *Neuron*. 79:814-828.
6. Dandash O, Fornito A, Lee J, Keefe RS, Chee MW, Adcock RA, et al. (2014): Altered striatal functional connectivity in subjects with an at-risk mental state for psychosis. *Schizophrenia bulletin*. 40:904-913.
7. Wotruba D, Michels L, Buechler R, Metzler S, Theodoridou A, Gerstenberg M, et al. (2014): Aberrant coupling within and across the default mode, task-positive, and salience network in subjects at risk for psychosis. *Schizophrenia bulletin*. 40:1095-1104.
8. Wang C, Ji F, Hong Z, Poh JS, Krishnan R, Lee J, et al. (2016): Disrupted salience network functional connectivity and white-matter microstructure in persons at risk for psychosis: findings from the LYRIKS study. *Psychological Medicine*. 46:2771-2783.
9. Manoliu A, Riedl V, Zherdin A, Muhlau M, Schwerthoffer D, Scherr M, et al. (2014): Aberrant dependence of default mode/central executive network interactions on anterior insular salience network activity in schizophrenia. *Schizophrenia bulletin*. 40:428-437.
10. Cauda F, D'Agata F, Sacco K, Duca S, Geminiani G, Vercelli A (2011): Functional connectivity of the insula in the resting brain. *Neuroimage*. 55:8-23.
11. Tian Y, Zalesky A (2018): Characterizing the functional connectivity diversity of the insula cortex: Subregions, diversity curves and behavior. *Neuroimage*. 183:716-733.
12. Cauda F, Costa T, Torta DM, Sacco K, D'Agata F, Duca S, et al. (2012): Meta-analytic clustering of the insular cortex: characterizing the meta-analytic connectivity of the insula when involved in active tasks. *Neuroimage*. 62:343-355.
13. Nanetti L, Cerliani L, Gazzola V, Renken R, Keysers C (2009): Group analyses of connectivity-based cortical parcellation using repeated k-means clustering. *Neuroimage*. 47:1666-1677.
14. Kelly C, Toro R, Di Martino A, Cox CL, Bellec P, Castellanos FX, et al. (2012): A convergent functional architecture of the insula emerges across imaging modalities. *Neuroimage*. 61:1129-1142.
15. Jakab A, Molnar PP, Bogner P, Beres M, Berenyi EL (2012): Connectivity-based parcellation reveals interhemispheric differences in the insula. *Brain topography*. 25:264-271.
16. Alcauter S, Lin W, Keith Smith J, Gilmore JH, Gao W (2015): Consistent anterior-posterior segregation of the insula during the first 2 years of life. *Cerebral cortex (New York, NY : 1991)*. 25:1176-1187.
17. Deen B, Pitskel NB, Pelphrey KA (2011): Three systems of insular functional connectivity identified with cluster analysis. *Cerebral cortex (New York, NY : 1991)*. 21:1498-1506.
18. Chang LJ, Yarkoni T, Khaw MW, Sanfey AG (2013): Decoding the role of the insula in human cognition: functional parcellation and large-scale reverse inference. *Cerebral cortex (New York, NY : 1991)*. 23:739-749.
19. Mutschler I, Wieckhorst B, Kowalevski S, Derix J, Wentlandt J, Schulze-Bonhage A, et al. (2009): Functional organization of the human anterior insular cortex. *Neuroscience letters*. 457:66-70.
20. Power JD (2011): Functional network organization of the human brain. *Neuron*. 72:665-678.
21. Yeo BT, Krienen FM, Sepulcre J, Sabuncu MR, Lashkari D, Hollinshead M, et al. (2011): The organization of the human cerebral cortex estimated by intrinsic functional connectivity. *Journal of neurophysiology*. 106:1125-1165.
22. Nelson SM, Dosenbach NU, Cohen AL, Wheeler ME, Schlaggar BL, Petersen SE (2010): Role of the anterior insula in task-level control and focal attention. *Brain structure*

and function. 214:669-680.
23. Glasser MF, Coalson TS, Robinson EC, Hacker CD, Harwell J, Yacoub E, et al. (2016): A multi-modal parcellation of human cerebral cortex. *Nature*. 536:171-178.
24. Yamada T, Itahashi T, Nakamura M, Watanabe H, Kuroda M, Ohta H, et al. (2016): Altered functional organization within the insular cortex in adult males with high-functioning autism spectrum disorder: evidence from connectivity-based parcellation. *Molecular autism*. 7:41.
25. Kurth F, Zilles K, Fox PT, Laird AR, Eickhoff SB (2010): A link between the systems: functional differentiation and integration within the human insula revealed by meta-analysis. *Brain structure & function*. 214:519-534.
26. Nomi JS, Farrant K, Damaraju E, Rachakonda S, Calhoun VD, Uddin LQ (2016): Dynamic Functional Network Connectivity Reveals Unique and Overlapping Profiles of Insula Subdivisions. *Human brain mapping*. 37:1770-1787.
27. Vercelli U, Diano M, Costa T, Nani A, Duca S, Geminiani G, et al. (2016): Node Detection Using High-Dimensional Fuzzy Parcellation Applied to the Insular Cortex. *Neural plasticity*. 2016:1938292.
28. Seeley WW, Menon V, Schatzberg AF, Keller J, Glover GH, Kenna H, et al. (2007): Dissociable intrinsic connectivity networks for salience processing and executive control. *Journal of Neuroscience*. 27:2349-2356.
29. Cole MW, Schneider W (2007): The cognitive control network: Integrated cortical regions with dissociable functions. *Neuroimage*. 37:343-360.
30. Cerliani L, Thomas RM, Jbabdi S, Siero JC, Nanetti L, Crippa A, et al. (2012): Probabilistic tractography recovers a rostrocaudal trajectory of connectivity variability in the human insular cortex. *Human brain mapping*. 33:2005-2034.
31. Ganella EP, Bartholomeusz CF, Seguin C, Whittle S, Bousman C, Phassouliotis C, et al. (2017): Functional brain networks in treatment-resistant schizophrenia. *Schizophrenia research*. 184:73-81.
32. Fornito A, Zalesky A, Pantelis C, Bullmore ET (2012): Schizophrenia, neuroimaging and connectomics. *Neuroimage*. 62:2296-2314.
33. Tan HY, Sust S, Buckholtz JW, Mattay VS, Meyer-Lindenberg A, Egan MF, et al. (2006): Dysfunctional prefrontal regional specialization and compensation in schizophrenia. *The American journal of psychiatry*. 163:1969-1977.
34. Howes OD, McCutcheon R, Agid O, de Bartolomeis A, van Beveren NJ, Birnbaum ML, et al. (2017): Treatment-Resistant Schizophrenia: Treatment Response and Resistance in Psychosis (TRRIP) Working Group Consensus Guidelines on Diagnosis and Terminology. *The American journal of psychiatry*. 174:216-229.
35. Sheehan DV, Lecrubier Y, Sheehan KH, Amorim P, Janavs J, Weiller E, et al. (1998): The Mini-International Neuropsychiatric Interview (M.I.N.I.): the development and validation of a structured diagnostic psychiatric interview for DSM-IV and ICD-10. *The Journal of clinical psychiatry*. 59 Suppl 20:22-33;quiz 34-57.
36. Kay SR, Fiszbein A, Opfer LA (1987): The positive and negative syndrome scale (PANSS) for schizophrenia. *Schizophrenia bulletin*. 13:261.
37. Andreasen N (1985): *The scale for the assessment of positive symptoms*. Iowa City: University of Iowa Press.
38. Andreasen NC (1989): Scale for the Assessment of Negative Symptoms (SANS). *The British Journal of Psychiatry*. 155:53-58.
39. Hall RC, Parks J (1995): The modified global assessment of functioning scale: addendum. *Psychosomatics*. 36:416-417.
40. Goldman HH, Skodol AE, Lave TR (1992): Revising axis V for DSM-IV: a review of measures of social functioning. *The American journal of psychiatry*. 149:1148-1156.

41. Wechsler D (2008): Wechsler adult intelligence scale‐Fourth Edition (WAIS‐IV). *San Antonio, TX: NCS Pearson*. 22:498.
42. Leucht S, Samara M, Heres S, Davis JM (2016): Dose Equivalents for Antipsychotic Drugs: The DDD Method. *Schizophrenia bulletin*. 42 Suppl 1:S90-94.
43. Winkler AM, Ridgway GR, Webster MA, Smith SM, Nichols TE (2014): Permutation inference for the general linear model. *NeuroImage*. 92:381-397.
44. Belkin M, Niyogi P (2003): Laplacian Eigenmaps for Dimensionality Reduction and Data Representation. *Neural Computation*. 15:1373-1396.
45. Haak KV, Marquand AF, Beckmann CF (2018): Connectopic mapping with resting-state fMRI. *Neuroimage*. 170:83-94.
46. Uddin LQ (2015): Salience processing and insular cortical function and dysfunction. *Nature reviews Neuroscience*. 16:55-61.
47. Kasai K, Shenton ME, Salisbury DF, et al. (2003): Progressive decrease of left heschl gyrus and planum temporale gray matter volume in first-episode schizophrenia: A longitudinal magnetic resonance imaging study. *Archives of general psychiatry*. 60:766-775.
48. Shinn AK, Baker JT, Cohen BM, Ongur D (2013): Functional connectivity of left Heschl's gyrus in vulnerability to auditory hallucinations in schizophrenia. *Schizophrenia research*. 143:260-268.
49. Morch-Johnsen L, Nesvag R, Jorgensen KN, Lange EH, Hartberg CB, Haukvik UK, et al. (2017): Auditory Cortex Characteristics in Schizophrenia: Associations With Auditory Hallucinations. *Schizophrenia bulletin*. 43:75-83.
50. Hotelling H (1936): Relations between two sets of variates. *Biometrika*. 28:321-377.
51. Xia M, Wang J, He Y (2013): BrainNet Viewer: A Network Visualization Tool for Human Brain Connectomics. *PloS one*. 8.
52. Ellison-Wright I, Glahn DC, Laird AR, Thelen SM, Bullmore E (2008): The anatomy of first-episode and chronic schizophrenia: an anatomical likelihood estimation meta-analysis. *The American journal of psychiatry*. 165:1015-1023.
53. Glahn DC, Laird AR, Ellison-Wright I, Thelen SM, Robinson JL, Lancaster JL, et al. (2008): Meta-analysis of gray matter anomalies in schizophrenia: application of anatomic likelihood estimation and network analysis. *Biological psychiatry*. 64:774-781.
54. Takahashi T, Wood SJ, Soulsby B, Tanino R, Wong MT, McGorry PD, et al. (2009): Diagnostic specificity of the insular cortex abnormalities in first-episode psychotic disorders. *Progress in neuro-psychopharmacology & biological psychiatry*. 33:651-657.
55. Takahashi T, Wood SJ, Yung AR, Phillips LJ, Soulsby B, McGorry PD, et al. (2009): Insular cortex gray matter changes in individuals at ultra-high-risk of developing psychosis. *Schizophrenia research*. 111:94-102.
56. Takahashi T, Wood SJ, Soulsby B, McGorry PD, Tanino R, Suzuki M, et al. (2009): Follow-up MRI study of the insular cortex in first-episode psychosis and chronic schizophrenia. *Schizophrenia research*. 108:49-56.
57. Tononi G, Sporns O, Edelman GM (1994): A measure for brain complexity: relating functional segregation and integration in the nervous system. *Proceedings of the National Academy of Sciences of the United States of America*. 91:5033-5037.
58. Cohen JR, D'Esposito M (2016): The Segregation and Integration of Distinct Brain Networks and Their Relationship to Cognition. *The Journal of neuroscience : the official journal of the Society for Neuroscience*. 36:12083-12094.
59. Fornito A, Zalesky A, Bullmore ET (2016): *Fundamental of brain network analysis*. 1st ed. U.S.A: Academic Press.
60. Taylor KS, Seminowicz DA, Davis KD (2009): Two systems of resting state connectivity between the insula and cingulate cortex. *Human brain mapping*. 30:2731-2745.
61. Cloutman LL, Binney RJ, Drakesmith M, Parker GJ, Lambon Ralph MA (2012): The

variation of function across the human insula mirrors its patterns of structural connectivity: evidence from in vivo probabilistic tractography. *Neuroimage*. 59:3514-3521.
62. Mesulam MM, Mufson EJ (1982): Insula of the old world monkey. I. Architectonics in the insulo-orbito-temporal component of the paralimbic brain. *The Journal of comparative neurology*. 212:1-22.
63. Mufson EJ, Mesulam MM (1982): Insula of the old world monkey. II: Afferent cortical input and comments on the claustrum. *The Journal of comparative neurology*. 212:23-37.
64. Kaufmann T, Skåtun KC, Alnæs D, Doan NT, Duff EP, Tønnesen S, et al. (2015): Disintegration of Sensorimotor Brain Networks in Schizophrenia. *Schizophrenia bulletin*. 41:1326-1335.
65. Keefe RS, Fenton WS (2007): How should DSM-V criteria for schizophrenia include cognitive impairment? *Schizophrenia bulletin*. 33:912-920.
66. Kohler CG, Walker JB, Martin EA, Healey KM, Moberg PJ (2010): Facial Emotion Perception in Schizophrenia: A Meta-analytic Review. *Schizophrenia bulletin*. 36:1009-1019.
67. Sotiropoulos SN, Zalesky A (2017): Building connectomes using diffusion MRI: why, how and but. *NMR in biomedicine*.
68. Menon V, Uddin LQ (2010): Saliency, switching, attention and control: a network model of insula function. *Brain structure & function*. 214:655-667.
69. Palaniyappan L, Liddle PF (2012): Does the salience network play a cardinal role in psychosis? An emerging hypothesis of insular dysfunction. *Journal of psychiatry & neuroscience : JPN*. 37:17-27.
70. Radua J, Borgwardt S, Crescini A, Mataix-Cols D, Meyer-Lindenberg A, McGuire PK, et al. (2012): Multimodal meta-analysis of structural and functional brain changes in first episode psychosis and the effects of antipsychotic medication. *Neuroscience & Biobehavioral Reviews*. 36:2325-2333.
71. Abbott CC, Jaramillo A, Wilcox CE, Hamilton DA (2013): Antipsychotic drug effects in schizophrenia: a review of longitudinal FMRI investigations and neural interpretations. *Current medicinal chemistry*. 20:428-437.
72. Schmidt A, Palaniyappan L, Smieskova R, Simon A, Riecher-Rossler A, Lang UE, et al. (2016): Dysfunctional insular connectivity during reward prediction in patients with first-episode psychosis. *Journal of psychiatry & neuroscience : JPN*. 41:367-376.
73. Miller GA, Chapman JP (2001): Misunderstanding analysis of covariance. *Journal of abnormal psychology*. 110:40-48.

Figure legends

Figure 1. Bipartite parcellation of the right insular cortex based on resting-state functional connectivity in individuals with schizophrenia and healthy comparison individuals. **Panel A:** Group consensus matrices (insula voxels × insula voxels) for the schizophrenia (upper matrix) and healthy comparison groups (lower). Each cell stores the proportion of individuals for which a given pair of insula voxels comprised the same cluster.

Warm tones (red) indicate pairs of voxels consistently comprising the same subregions, whereas cool tones (blue) indicate pairs of voxels consistently comprising distinct subregions. While two modules were identified in both groups, modular separation was significantly reduced in the schizophrenia group (Q=0.13, P=0.0038), compared to the healthy comparison group (Q=0.20). The rows/columns of the consensus matrices are ordered such that all insula voxels comprising the anterior insula module are listed first, followed by all voxels in the posterior insula. **Panel B:** The consensus matrices are mapped to the insula to yield probabilistic maps of the anterior and posterior insula subregions. The color of each insula voxel is modulated by the proportion of individuals for which the voxel comprised the relevant subregion (module). Yellow tones indicate voxels that consistently comprise the relevant subregion across individuals, whereas red tones indicate voxels that rarely comprise the subregion. Probability maps were converted to binary (hard) segmentations to delineate discrete anterior (yellow) and posterior (red) insula subregions for both groups. **Panel C:** The intersection of the anterior insula subregion delineated for each of the two groups was determined to define a consensus anterior insula subregion for both groups (green), and similarly for the posterior insula subregion (pink). Slice coordinates (MNI, mm): x=40, y=−10, z=2.

Figure 2. **Altered resting-state functional connectivity of the anterior and posterior insular cortex in schizophrenia.** Functional connectivity was mapped between the anterior and posterior insula subregions and all other gray matter voxels. Analysis of variance (ANOVA) was then used to test the main effect of subregion (anterior vs posterior) and diagnosis (schizophrenia vs healthy comparison group) on insula connectivity at each gray matter voxel, as well as the interaction between these two main effects. **Panel A:** Main effect of subregion. The anterior and posterior insula subregions showed unique connectivity

patterns: The anterior insula was preferentially connected to frontal-limbic areas and the posterior cerebellar lobe, whereas the posterior insula was characterized by increased connectivity with the parietal-temporal-occipital cortices and anterior cerebellar. **Panel B:** Main effect of diagnosis. Schizophrenia was associated with significant reductions in connectivity between the insula and multiple cortical/subcortical areas, relative to the healthy comparison group. Connectivity increases were not evident in the schizophrenia group. **Panel C:** Interaction effect. A significant interaction between subregion and diagnosis was found: The anterior insula subregion showed increased connectivity with the somatosensory/motor and occipital cortex in the schizophrenia group, whereas connectivity between the posterior insula and prefrontal cortex and thalamus was increased in schizophrenia. AI: anterior insula; PI: posterior insula; SCZ: schizophrenia group; CON: healthy comparison group. Clusters are coloured according to t-statistic. All images pertain to right insula.

Figure 3. Diversity curves for the insular cortex in schizophrenia. Panel A: Group-averaged insula diversity curves for the schizophrenia (green curve) and healthy comparison (blue) groups. Dashed box indicates the portion of the diversity curve showing a significant reduction in the schizophrenia group ($p<0.05$, uncorrected). Shading denotes 95% confidence intervals (CI). **Panel B:** Group-consensus eigenmap values were mapped to the voxels of the insula to enable anatomical visualization of variation in connectional diversity for the schizophrenia (lower panel) and healthy comparison (upper) groups. The streamlines superposed onto the anatomical images were previously computed as part of a previous study (40). Diversity curves were mapped by projecting each individual's eigenmap onto the longest streamline (solid red line). Arrows indicate the gradient direction estimated for each voxel and the lengths convey gradient magnitude.

Figure 4. Association between insula functional connectivity and inter-individual variation in clinical characteristics. Canonical correlation analysis (CCA) identified a significant mode of covariance between inter-individual variation in two measures of insula functional connectivity and nine measures of disorder severity, including measures of cognition, psychosocial functioning, psychotic symptoms and duration of illness. **Panel A:** Scatter plot of canonical scores for the functional connectivity measures (horizontal axis) and measures of disorder severity (vertical axis). The mode of covariance remained significant after correction for multiple comparisons (r=0.64, p=0.03; familywise error corrected across all CCA modes with permutation testing, n=10,000). **Panel B:** Bar plot showing canonical coefficients for the functional connectivity strengths corresponding to: i) right anterior insula (rAI) and ACC/SMA (cyan cluster, 0.57); and ii) right posterior insula (rPI) and STG (blue cluster, 0.71). **Panel C:** Bar plot showing correlation coefficients between the nine measures of disorder severity and the significant CCA mode. Measures with positive canonical coefficients are positively correlated with the CCA mode of variance. Therefore, increased insula functional connectivity is associated with increased IQ, GAF and SOFAS, but decreased SANS, PANSS-NEG and DOI. Red asterisks indicate measures that are significantly correlated with the canonical score (FDR corrected). IQ: intelligence quotient; GAF: global assessment of functioning; SOFAS: social and occupational functioning assessment scale; SAPS: scale for assessment of positive symptoms; SANS: scale for assessment of negative symptoms; PANSS-POS: PANSS positive scale; PANSS-NEG: PANSS negative scale; PANSS-GEN: PANSS general psychopathology scale; DOI: duration of illness.

Table 1. Demographic and clinical characteristics

	Schizophrenia group (*N*=49)	**Comparison group** (*N*=52)	**Statistic**	**p-value**
Age (year)	41.02 (9.93)	39.85 (10.46)	t=0.58	0.56
Sex (M/F)	34/15	35/17	χ^2=0.05	0.82
Handedness (R/L)	45/4	50/2	χ^2=0.84	0.36
Current IQ	91.34 (18.70)	111.51 (14.04)	t=5.91	< 0.001
GAF	47.85 (13.50)	79.27 (11.34)	t=12.52	< 0.001
SOFAS	48.38 (14.81)	79.44 (11.63)	t=11.66	< 0.001
Age of illness onset	22.71 (6.44)	-	-	-
Duration of illness	17.95 (9.16)	-	-	-
PANSS-P	16.08 (5.72)	-	-	-
PANSS-N	18.5 (7.90)	-	-	-
PANSS-G	22.25 (9.72)	-	-	-
PANSS-T	51.32 (24)	-	-	-
SAPS	20.37 (16.31)			
SANS	40.60 (19.28)			
Clozapine dosage (mg/d)	383.70 (134.20)	-	-	-
CPZ equivalent (mg/d)	498.80 (281.10)			

IQ, intellectual quotient; GAF, Global Assessment of Functioning; SOFAS, Social and Occupational Functioning Assessment Scale; PANSS-P, PANSS score for positive symptoms; PANSS-N, PANSS subtotal score for negative symptoms; PANSS-G, PANSS subtotal score for general psychopathology; PANSS-T, total PANSS score. SAPS: Scale for the Assessment of Positive Symptoms total score. SANS: Scale for the Assessment of Negative Symptoms total score. Values are given as mean (SD) except where noted. CPZ, Chlorpromazine.

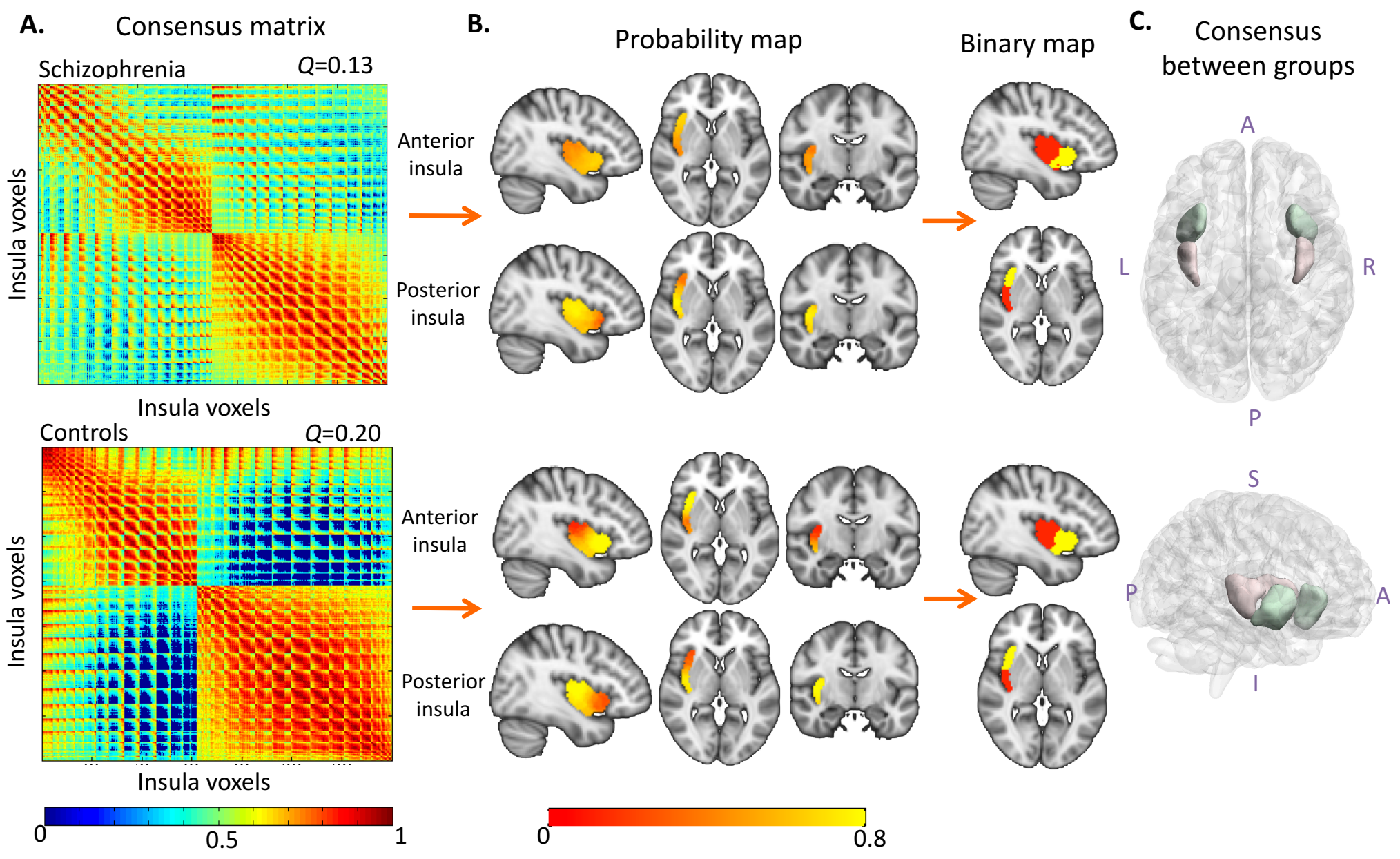
A.
Consensus matrix
Schizophrenia
Q=0.13
Insula voxels
Insula voxels
Controls
Q=0.20
Insula voxels
Insula voxels
0
0.5
1
B.
Probability map
Binary map
Anterior insula
Posterior insula
Anterior insula
Posterior insula
0
0.8
C.
Consensus between groups
A
L
R
P
S
P
A
I

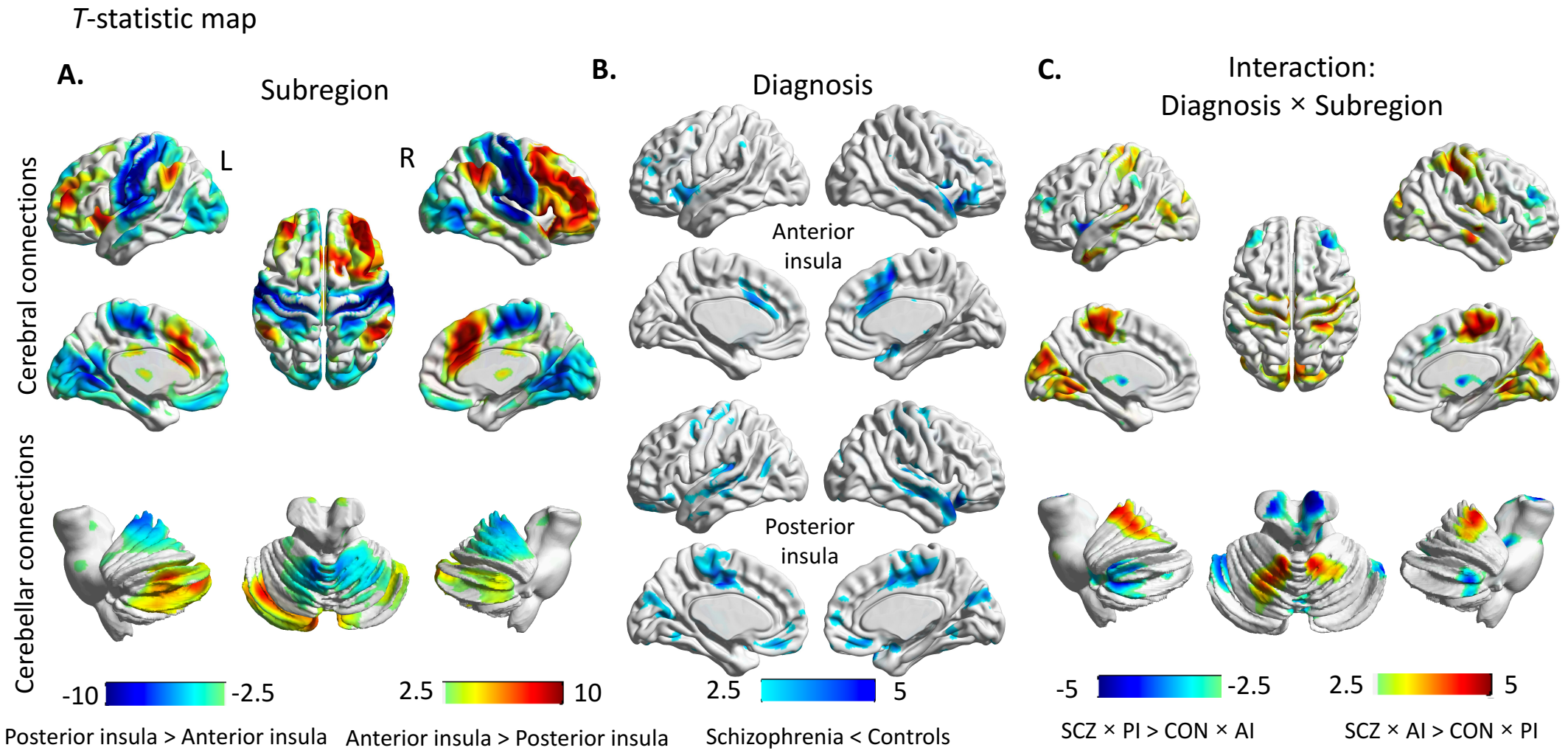
T-statistic map
A.
Subregion
B.
Diagnosis
C.
Interaction:
Diagnosis × Subregion
Cerebral connections
Cerebellar connections
L
R
Anterior insula
Posterior insula
-10
-2.5
2.5
10
2.5
5
-5
-2.5
2.5
5
Posterior insula > Anterior insula
Anterior insula > Posterior insula
Schizophrenia < Controls
SCZ × PI > CON × AI
SCZ × AI > CON × PI

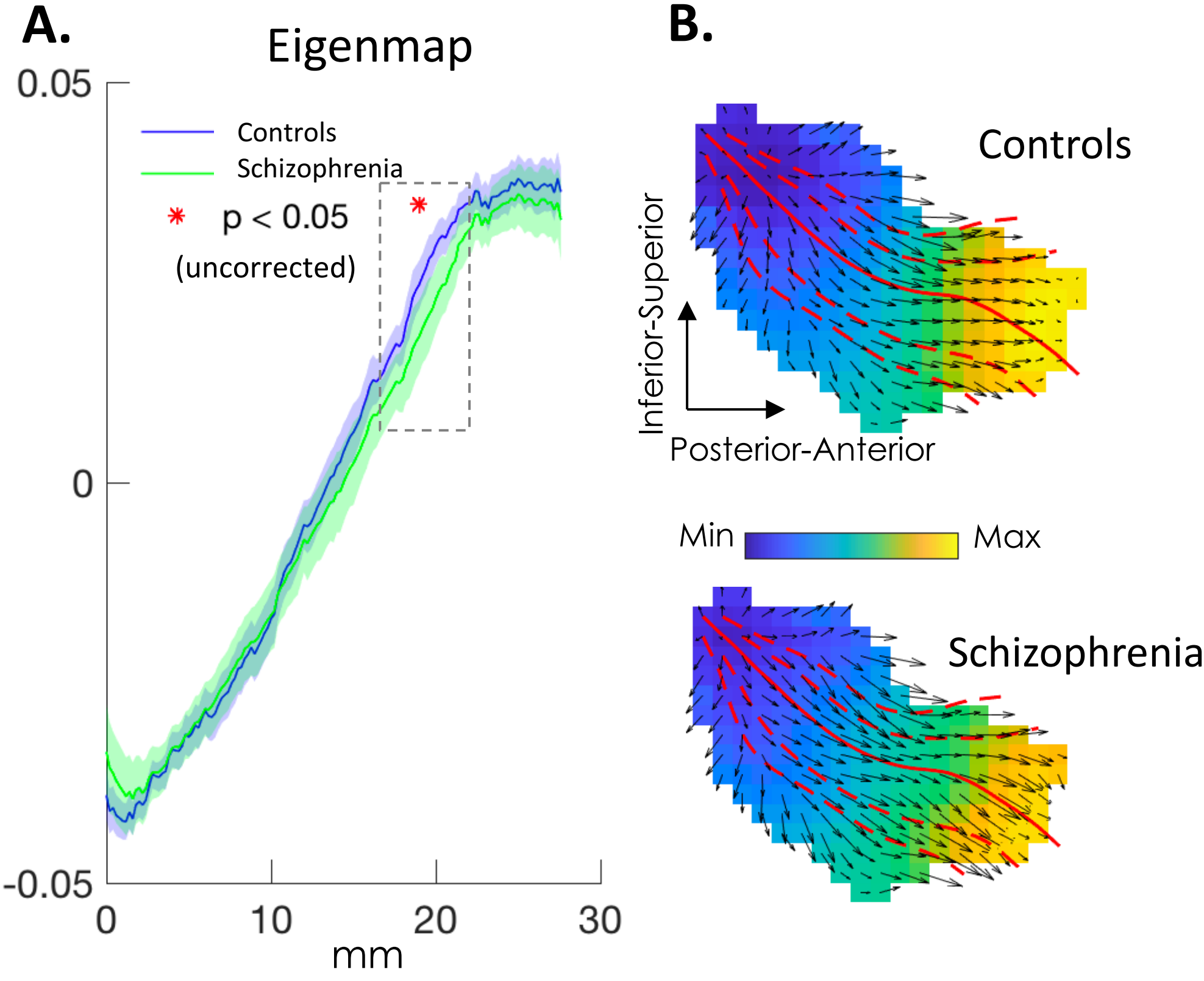
A.
Eigenmap
0.05
0
-0.05
Controls
Schizophrenia
p < 0.05
(uncorrected)
0
10
20
30
mm
B.
Controls
Inferior-Superior
Posterior-Anterior
Min
Max
Schizophrenia

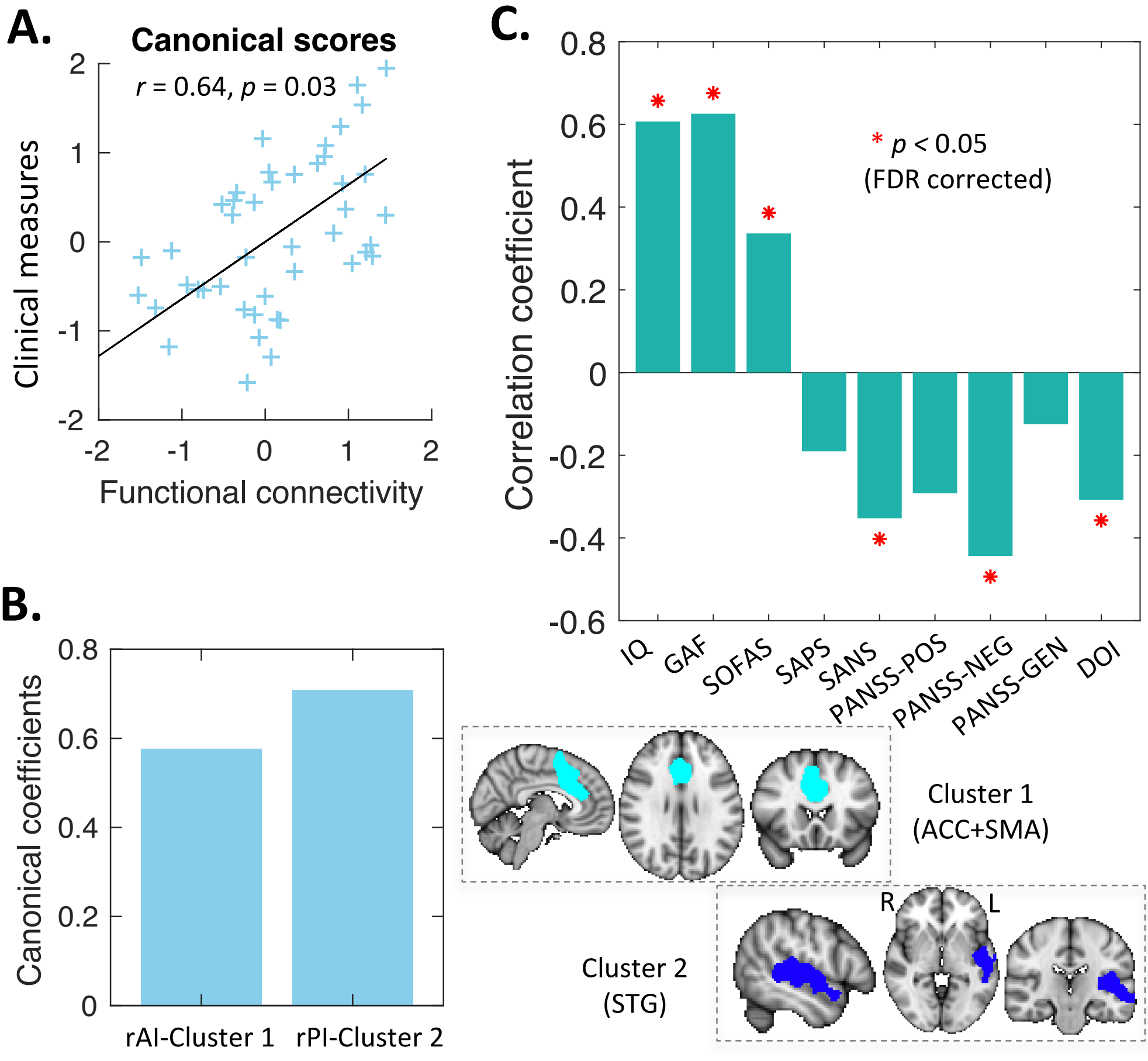
A.
Canonical scores
r = 0.64, p = 0.03
Clinical measures
Functional connectivity
B.
Canonical coefficients
rAI-Cluster 1
rPI-Cluster 2
C.
Correlation coefficient
* p < 0.05
(FDR corrected)
IQ
GAF
SOFAS
SAPS
SANS
PANSS-POS
PANSS-NEG
PANSS-GEN
DOI
Cluster 1
(ACC+SMA)
Cluster 2
(STG)
R
L

Insula Functional Connectivity in Schizophrenia: Subregions, Gradients and Symptoms

Supplementary Information

Table of Contents

Image Acquisition and Resting-state fMRI Data Preprocessing

Image Acquisition: Imaging was performed in all participants using a Siemens Avanto 3T Magnetom TIM Trio scanner. Structural images of brain anatomy were acquired using an optimized Magnetization-Prepared Rapid Acquisition Gradient Echo (MPRAGE) T1-weighted sequence with 176 sagittal slices of 1.2mm thickness; field of view (FOV) = 256×256 mm^2; flip angle = 9°; repetition time (TR) = 2300ms; echo time (TE) = 2.98ms; voxel size =1.0×1.0×1.2 mm^3. Resting-state fMRI was acquired using a T2*-weighted echo-planar imaging sequence. A total of 8 min of resting-state data was acquired, resulting in 234 volumes (TR = 2000ms; TE = 32.0ms; voxel size = 3.3×3.3×3.5 mm^3).

Resting-state fMRI Data Preprocessing: Resting-state fMRI data were preprocessed using FSL 5.0.8 (http://fsl.fmrib.ox.au.uk/fsl/fslwiki/). In brief, preprocessing steps included: slice-timing correction; brain extraction; linear registration of all volumes to the middle volume to correct for intrascan head motion; warping of all volumes to MNI space and resampling to 2mm isotropic voxels. These steps were performed independently for each individual. Motion artefacts were further corrected with ICA-AROMA (v0.3-beta, ICA-based automatic removal of motion artefacts) after spatial smoothing with a Gaussian kernel of 4mm FWHM (full width at half maximum). ICA-AROMA is a data-driven method to identify and automatically remove motion-related variance (1, 2). For each voxel, the preprocessed fMRI data was then regressed against the motion-related components identified with ICA-AROMA, together with mean white matter and cerebrospinal fluid signals (CSF). The residuals of this regression were temporally band-pass filtered (0.01-0.1 Hz) and used in all further analyses.

Cluster Analysis

Binary insula masks were delineated based on the Harvard-Oxford Cortical Structural Atlas (https://fsl.fmrib.ox.ac.uk/fsl/fslwiki/Atlases) using a probability threshold of 20%, resulting in 1399 voxels (11.19cm^3) for right insula and 1397 voxels (11.17cm^3) for left insula. The fMRI signal at each insula voxel was correlated (Pearson correlation) with all other gray matter voxels, yielding a voxel-wise functional connectivity matrix (*r*-to-*z* transformed) of dimension $N \times M$, where N denotes the number of insula voxels and M denotes the number of all other gray matter voxels. Principal component analysis (PCA) was then applied to the z-transformed connectivity matrix. These steps were performed independently for each individual and the top three principal components were found to explain more than 80% of the variance across gray matter voxels for each individual. The Euclidean distance between all pairs of insula voxels was computed in this three-dimensional space ($N \times 3$), yielding a symmetric distance matrix of dimension $N \times N$. Ward's linkage (3) was then applied to this distance matrix to partition insula voxels into groups that shared similar connectivity patterns and connected to the same cortical and subcortical areas. To determine the most parsimonious number of clusters (subregions) comprising the insula, we used the W^{norm} cluster evaluation measure (4), which quantifies the normalized intra-to-inter-cluster distance. Specifically, we generated fMRI-specific null data to

compare W^{norm} with its expected value under the null hypothesis of no insula clusters. This approach has been shown to outperform classic cluster evaluation criteria when applied to fMRI data (4). Clusters were delineated independently for the right and left insula and for each individual.

Group-level Consensus Parcellation

For each of the two groups, an $N \times N$ consensus matrix was formed in which cell (i, j) was populated with the proportion of individuals for which voxels i and j resided in the same cluster. Newman's spectral community detection algorithm (5, 6) was then applied to each consensus matrix in an iterative manner (7) to yield a consensus parcellation. Each module in the consensus parcellation delineated an insula subregion. The modularity Q score was used to quantify the extent to which the consensus parcellation was modular (5, 8). Higher values of Q indicated stronger separation between putative insula subregions and/or increased consistency in the morphology of subregions across individuals. We used permutation testing to assess the null hypothesis of equality in Q scores between the schizophrenia and healthy comparison groups. Individuals were randomly permuted between the two groups and a consensus parcellation was computed for each group, as well as corresponding Q scores. This was repeated for 5000 permutations and the absolute difference between Q scores ($\Delta \mathrm{Q} = |Q_1 - Q_2|$) was stored for each permutation to generate an empirical null distribution that denoted the difference. The p-value was given by the proportion of permutations for which ΔQ exceeded or equalled the value of ΔQ in the true (unpermuted) groups.

Diversity Curves and Continuum Model

Laplacian eigenmaps for the insula were mapped using the procedure described by Haak et al. (9). Diversity curves were mapped as described by Tian and Zalesky (4). Given that the temporal and spatial resolution of the fMRI data used in this study was lower than the data analyzed in these two previous studies, we implemented the following additional procedures to assist in alleviating the effects of noise:

I. Rather than globally thresholding the similarity graph to yield the minimum connection density required to ensure a single connected component in the graph, we instead used the disparity filter (10) to perform thresholding. The disparity filter is a local thresholding method that may provide greater robustness to the effects of noisy edges. The significance level for the disparity filter was set independently for each individual according to the minimum connection density required to yield a single connected component. This resulted in graphs with connection densities of 5-28% across individuals.

II. The eigendecomposition described in Haak et al. (9) was performed on the symmetric normalized Laplacian matrix rather than the unnormalized Laplacian matrix. When visualized in the anatomical space of the insula, this yielded eigenmaps that were visibly less noisy.

Clinical Measures and Canonical Correlation Analysis

The following measures were included in the canonical correlation analysis (CCA): PANSS, SAPS, SANS, GAF, SOFAS, WASI and duration of illness (DOI). For each measure, scores were not available for between 0% and 6% of the individuals (missing data). For PANSS, an average item score across each of the subscales (ignoring the missing values) was calculated, yielding mean score for positive (PANSS-POS), negative (PANSS-NEG) and general psychopathology (PANSS-GEN) symptoms for each individual. Similarly, mean scores for SAPS and SANS, ignoring the missing values were computed. This mean score approach avoided potential underestimation of the severity of psychotic symptoms when item scores were summed in the presence of missing data. For GAF, SOFAS and WASI, missing values were replaced with nearest neighbor values based on Euclidean distance. DOI was recorded for all individuals. The sum of item scores for each measure is provided in Table 1 (ignoring individuals with missing values).

CCA was then used to test whether inter-individual variation in clinical features was associated with insula functional connectivity. In this study, one group of variables comprised 9 clinical measures, while the other group comprised the functional connectivity strength between insula subregion and regions (clusters) that were found to show significant between-group differences. The two groups of variables were submitted to the CCA function (*canoncorr*) available in *MATLAB*. The familywise error (FWE) was controlled with permutation testing. For each of the permutations (n=10,000), clinical measures were randomly permuted among individuals and CCA was repeated for the permuted data. The FWE corrected p-value for each CCA mode was given by the proportion of permutations with a maximum correlation coefficient that exceeded or equaled the mode's correlation in the unpermuted data. $p < 0.05$ was considered statistically significant.

Supplementary Figures

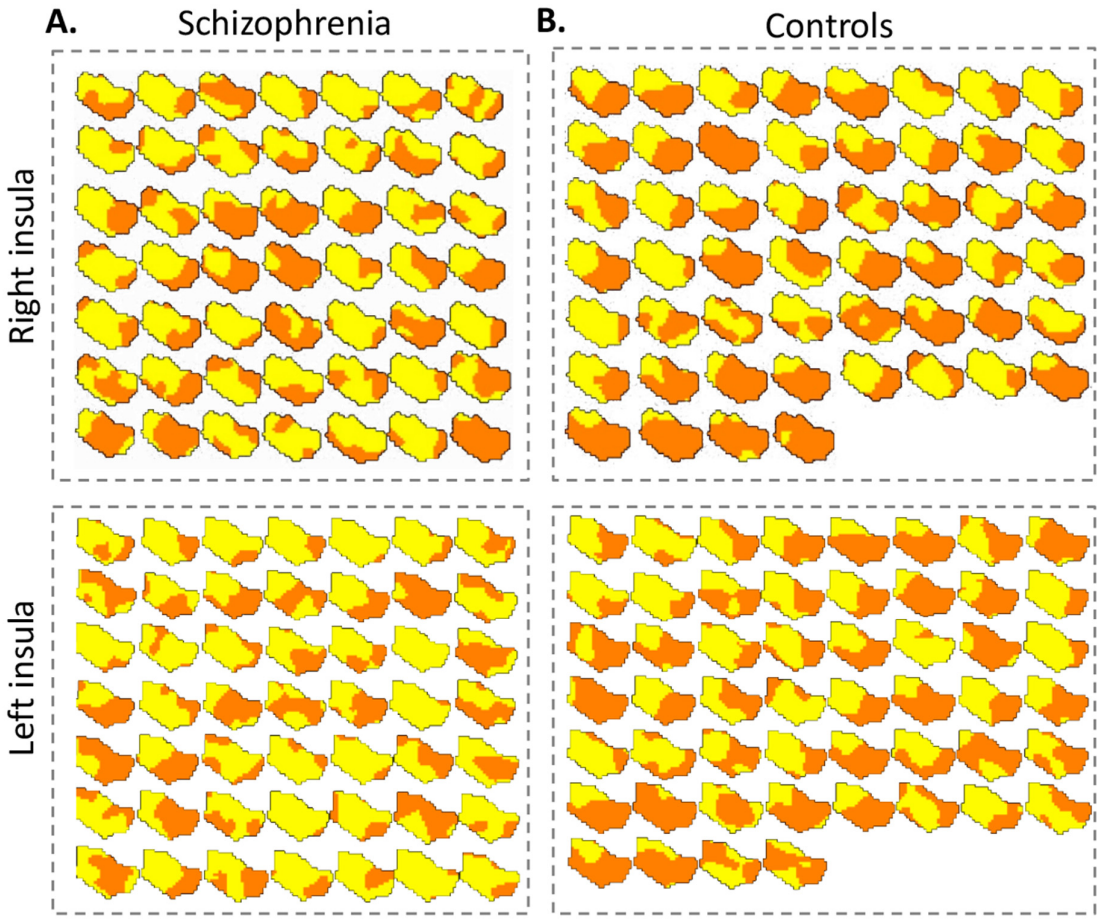

Figure S1. Individual bipartite parcellation of the insula based on resting-state functional connectivity in individuals with schizophrenia and healthy comparison individuals. Functional connectivity was mapped between each insula voxel and all other gray matter voxels, resulting in a whole-brain connectivity fingerprint for each insula voxel. Cluster analysis (*Ward's* linkage) was used to partition insula voxels that shared similar connectivity fingerprints into two clusters. Clusters were delineated independently in right (upper) and left insula (bottom) for each subject. The discrete subregions were mapped for each healthy comparison individual (Panel **A**) and each individual with schizophrenia (Panel **B**). For each individual, the cluster that overlapped to the greatest extent with the group-level segmented anterior insula (see Figure 1) was colored with orange. The other cluster was colored yellow. Note the significant variation across individuals in the shape and location of the two-putative insula subregions. Slice coordinates (MNI152, mm): right insula: x=38, y=0, z=8; left insula: x=−38, y=0, z=8.

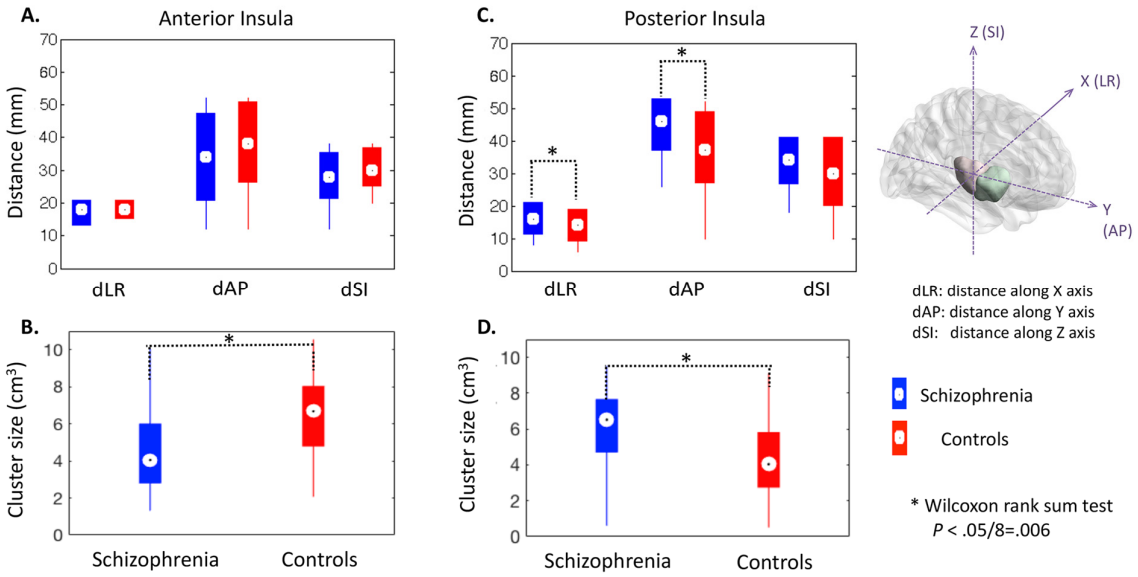

Figure S2. Comparison of cluster shape between schizophrenia and healthy comparison groups. Cluster analysis indicated that the left and right insula each comprise two subregions in both groups. For the schizophrenia group, the size of right anterior insula was smaller (z=3.81, p <0.0001, Panel **B**), while right posterior insula was larger (z=3.58, p <0.001, Panel **D**) and extended further anteriorly (z=3.44, p <0.001) and laterally (z=3.89, p <0.001, Panel **C**). Similar abnormalities were observed on the left side. Bonferroni correction was used for controlling for multiple comparison for the eight variables.

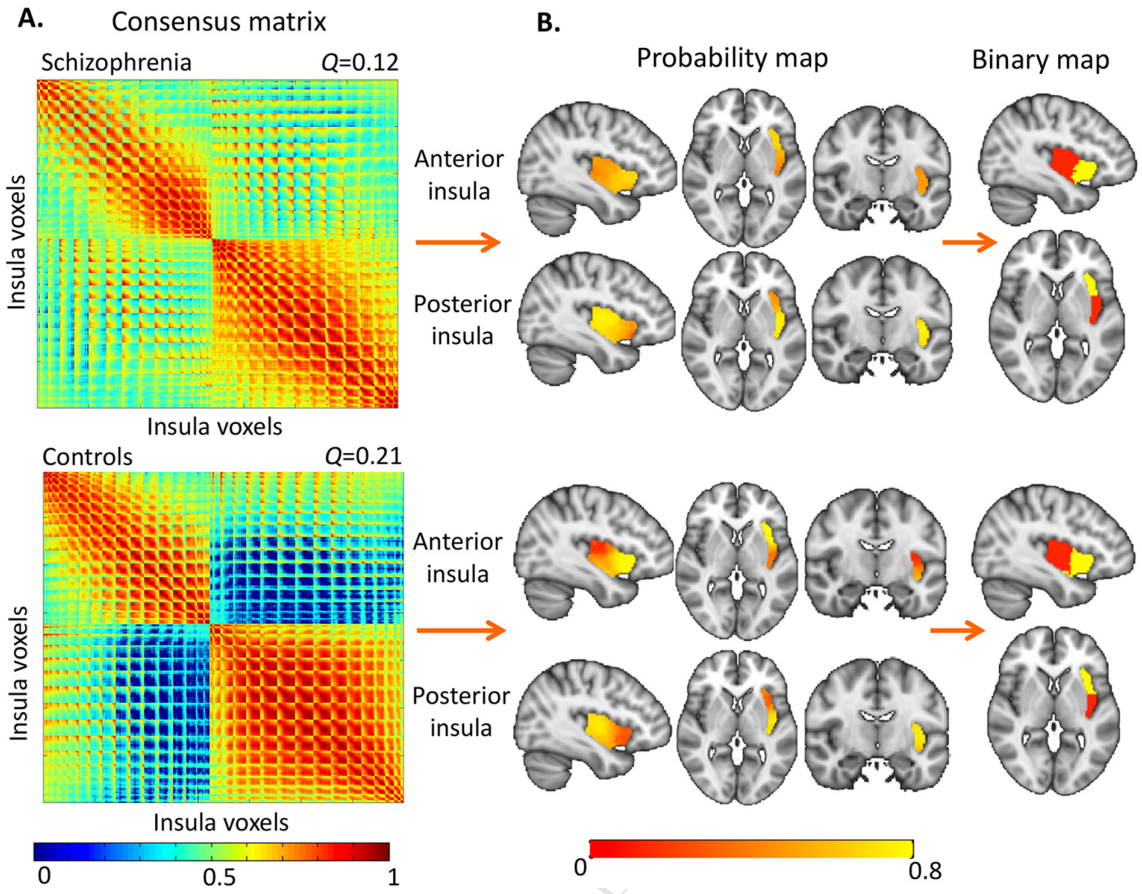

Figure S3. Bipartite parcellation of the left insula cortex based on resting-state functional connectivity in individuals with schizophrenia and healthy comparison individuals.

Panel A: Group consensus matrices (insula voxels × insula voxels) for the schizophrenia (upper matrix) and healthy comparison groups (lower). Each cell stores the proportion of individuals for which a given pair of insula voxels comprised the same cluster. Warm tones (red) indicate pairs of voxels consistently comprising the same subregions, whereas cool tones (blue) indicate pairs of voxels consistently comprising distinct subregions. While two modules were identified in both groups, modular separation was significantly reduced in the schizophrenia group (Q = 0.12, P = 0.002), compared to the healthy comparison group (Q = 0.21). The rows/columns of the consensus matrices are ordered such that all insula voxels comprising the anterior insula module are listed first, followed by all voxels in the posterior insula. **Panel B:** The consensus matrices are mapped to the insula to yield probabilistic maps of the anterior and posterior insula subregions. The color of each insula voxel is modulated by the proportion of individuals for which the voxel comprised the relevant subregion (module). Yellow tones indicate voxels that consistently comprise the relevant subregion across individuals, whereas red tones indicate voxels that rarely comprise the subregion. Probability maps were converted to binary (hard) segmentations to delineate discrete anterior (yellow) and posterior (red) insula subregions for both groups. The intersection of the anterior insula subregions delineated for each of the two groups was

determined to define a consensus anterior insula subregion for both groups (green), and similarly for the posterior insula subregion (pink) (see Figure 1, Panel C). Slice coordinates (MNI152, mm): x=−38, y=−10, z=2.

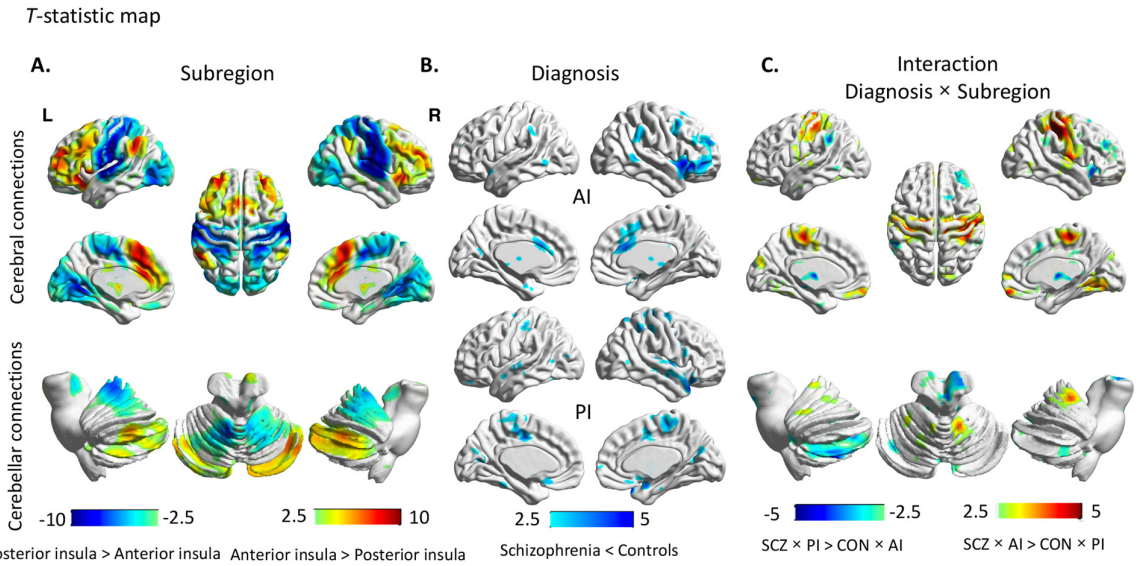

Figure S4. Altered resting-state functional connectivity of left anterior and posterior insula in schizophrenia. Functional connectivity was mapped between the anterior and posterior insula subregion and all other gray matter voxels. Analysis of variance was formulated to test the main effect of subregion (anterior vs posterior) and diagnosis (schizophrenia vs healthy comparison group) on insula connectivity at each gray matter voxel, as well as the interaction between these two main effects. **Panel A:** Main effect of subregion. The anterior and posterior insula subregions showed unique connectivity patterns: The anterior insula was preferentially connected to frontal-limbic areas and the posterior cerebellar lobe, whereas the posterior insula was characterized by increased connectivity with the parietal-temporal-occipital cortices and anterior cerebellar. **Panel B:** Main effect of diagnosis. Schizophrenia was associated with significant reductions in connectivity between the insula and multiple cortical/subcortical areas, relative to the healthy comparison group. Connectivity increases were not evident in the schizophrenia group. **Panel C:** Interaction effect. A significant interaction between subregion and diagnosis was found: The anterior insula subregion showed increased connectivity with the somatosensory/motor and occipital cortex in the schizophrenia group, whereas connectivity between the posterior insula and prefrontal cortex was increased in schizophrenia. AI: anterior insula; PI: posterior insula; SCZ: schizophrenia group; CON: healthy comparison group. Clusters are coloured according to t-statistic. All images pertain to left insula.

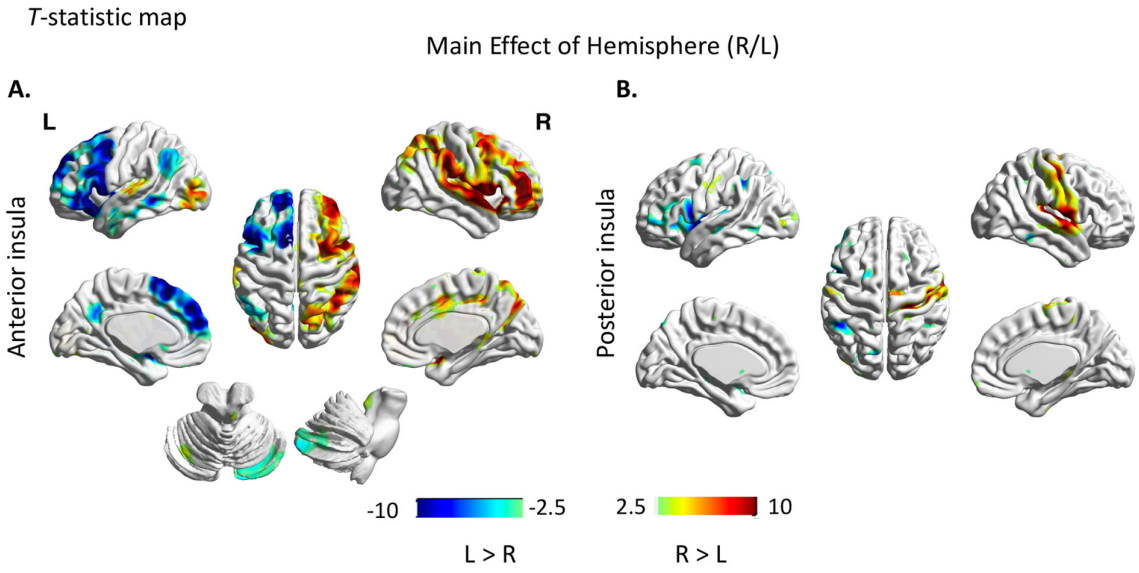

Figure S5. The main effect of hemisphere in resting-state functional connectivity of anterior and posterior insula cortex. An analysis of variance (ANOVA) was formulated to test the main effect of hemisphere (right and left) and diagnosis (controls and patients) on connectivity at each gray matter voxel. The interaction between hemisphere and diagnosis was also tested. The cerebral and cerebellar connections of insula cortex were bilateral and hemisphere preference was noted. While the cerebral connections showed an ipsilateral preference for both anterior insula (Panel **A**) and posterior insula (Panel **B**), cerebellar connections to anterior insula was more extensively connected to the cerebellum at the contralateral hemisphere (Panel **A**). No significant interaction was detected in contrast to diagnosis. Clusters are colored according to t-statistic.

Supplementary Tables

Table S1.
Information of group-level insula sub-regions, in MNI152 standard anatomical space.

Insula subregions	Healthy comparison group				Schizophrenia				Intersection			
	Cluster size (cm^3)	Mean coordinates (mm)			Cluster size (cm^3)	Mean coordinates (mm)			Cluster size (cm^3)	Mean coordinates (mm)		
		X	y	z		x	y	z		x	y	z
Right AI	6.24	35	14	-2	5.58	34	16	-2	5.48	34	16	-4
Right PI	4.94	35	-8	6	5.62	36	-6	6	4.85	36	-8	8
Left AI	6.00	-38	14	-2	5.42	-38	14	-2	5.28	-36	16	-2
Left PI	5.17	-40	-8	6	5.76	-40	-6	6	5.03	-40	-8	6

AI: anterior insula
PI: posterior insula

Table S2.
Anatomical locations of clusters associated with significantly reduced functional connectivity with insula subregions in the schizophrenia group, relative to the group of healthy comparison individuals (p<0.05, corrected). Clusters are shown in MNI152 standard anatomical space.

Clusters	Mean coordinates (COG, mm)			Anatomical visualization	Hemisphere	Peak t-stats	P-value	Seed region
	x	y	z					
Cluster 1	3.22	18	37.6	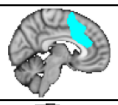	_	5.51	0.0118	Right AI
Cluster 2	-49	-17.5	0.78	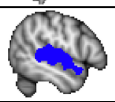	Left	4.59	0.0091	Right PI
Cluster 3	38.7	11.2	-10.1		Right	5.7	0.0035	Right AI
Cluster 4	36.5	7.06	-9.83	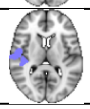	Right	5.31	0.0018	Right PI
Cluster 5	-4.62	-15.9	56.1		_	5.4	0.0018	Right PI
Cluster 6	38.3	28.2	0.1	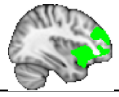	Right	5.66	0.0049	Left AI
Cluster 7	45.8	0.38	-8.48	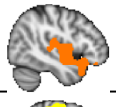	Right	5.35	0.0087	Left PI
Cluster 8	6.12	-17.3	59.8		_	4.69	0.0081	Left PI

COG, centre of gravity; AI, anterior insula; PI, posterior insula

Table S3.
Association between insula functional connectivity and age, sex and CPZ equivalent.

Clusters	FC-AGE		FC-SEX		FC-CPZ	
	r	p	t-stats	p	r	p
Cluster 1	-0.1598	0.2779	0.9843	0.3302	-0.1418	0.3364
Cluster 2	-0.0942	0.5242	1.4357	0.158	0.0269	0.8559
Cluster 3	-0.0971	0.5115	1.2292	0.2254	-0.0474	0.7491
Cluster 4	0.0714	0.6294	1.8223	0.0751	0.0108	0.9422
Cluster 5	0.102	0.4901	-0.0074	0.9942	-0.0775	0.6005
Cluster 6	-0.1451	0.3251	1.1861	0.2418	-0.1584	0.2823
Cluster 7	-0.0004	0.9977	-0.6698	0.5064	0.0366	0.805
Cluster 8	0.1171	0.4282	0.9187	0.3632	0.1559	0.29

FC, functional connectivity; CPZ, chlorpromazine.

Supplementary References

1. Pruim RHR, Mennes M, Buitelaar JK, Beckmann CF (2015): Evaluation of ICA-AROMA and alternative strategies for motion artifact removal in resting state fMRI. *NeuroImage*. 112:278-287.
2. Pruim RHR, Mennes M, van Rooij D, Llera A, Buitelaar JK, Beckmann CF (2015): ICA-AROMA: A robust ICA-based strategy for removing motion artifacts from fMRI data. *NeuroImage*. 112:267-277.
3. Ward J, Joe H (1963): Hierarchical grouping to optimize an objective function. *Journal of the American statistical association*. 58:236-244.
4. Tian Y, Zalesky A (2018): Characterizing the functional connectivity diversity of the insula cortex: Subregions, diversity curves and behavior. *Neuroimage*. 183:716-733.
5. Newman ME, Mark E (2006): Modularity and community structure in networks. *Proceedings of the National Academy of Sciences of the United States of America*. 103:8577-8582.
6. Newman ME (2013): Spectral methods for community detection and graph partitioning. *Physical Review E*. 88:042822.
7. Lancichinetti A, Fortunato S (2012): Consensus clustering in complex networks. *Scientific Reports*. 2:336.
8. Clauset A, Newman MEJ, Moore C (2004): Finding community structure in very large networks. *Physical Review E*. 70:066111.
9. Haak KV, Marquand AF, Beckmann CF (2018): Connectopic mapping with resting-state fMRI. *Neuroimage*. 170:83-94.
10. Serrano MÁ, Boguñá M, Vespignani A (2009): Extracting the multiscale backbone of complex weighted networks. *Proceedings of the National Academy of Sciences*. 106:6483-6488.